ELSEVIER

Volume 182, Number 1, January 2009

JOURNAL OF SOLID STATE CHEMISTRY

www.elsevier.com/locate/jssc

CONTENTS

Abstracted/indexed in BioEngineering Abstracts, Chemical Abstracts, Coal Abstracts, Current Contents/Physics, Chemical, & Earth Sciences, Engineering Index, Research Alert, SCISEARCH, Science Abstracts, and Science Citation Index. Also covered in the abstract and citation database SCOPUS®. Full text available on ScienceDirect®.

Regular Articles

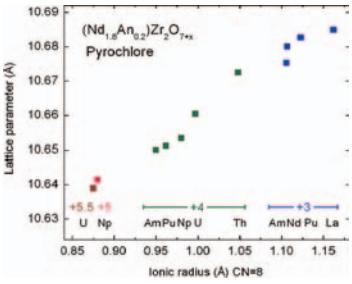

$(Nd_{1.8}An_{0.2})Zr_2O_{7+x}$ pyrochlore lattice parameter depending on the actinide, La, and Nd ionic radii in eightfold coordination.

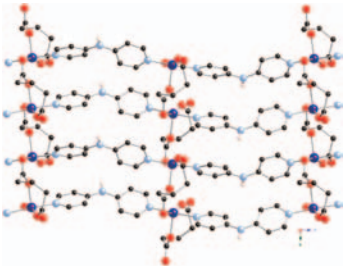

The coordination polymers $[M(glu)(dpa)]_n$ (M = Co (**1**), Ni (**2**), Cu (**3**); glu = glutarate, dpa = 4,4'-dipyridylamine) exhibit 2D layer structures based on 1D $[M(glu)]_n$ chains linked through dpa tethers. Antiferromagnetic coupling is observed for **2** and **3**, while ferromagnetism is predominant in **1**. Compound **3** undergoes a thermally induced single crystal-to-single crystal transformation from an acentric to a centrosymmetric space group.

Regular Articles—Continued

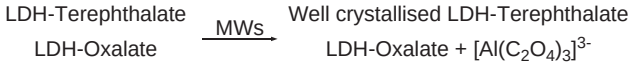

The influence of the nature of the interlayer anion during the ageing process of carboxylate-intercalated (TA and ox) hydrotalcite-like compounds (HTlcs) is studied. Well crystallized for TA-containing compounds were obtained. However, the non-desired side-reaction of ox with the aluminum of the layers is enhanced by the microwaves and a partial destruction of the structure takes place.

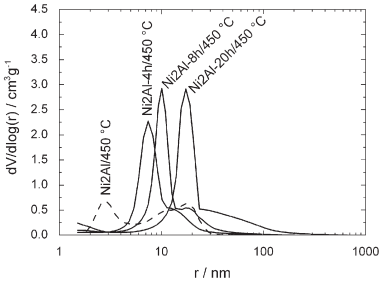

Hydrothermal treatment of Ni–Al LDH precursors influenced the porous structure of related mixed oxides and considerably improved their catalytic activity in N_2O decomposition; the higher catalytic activity of hydrothermally treated samples can be explained by suppressing internal diffusion effect in catalysts grains.

Continued

Thin $La_2Zr_2O_7$ films made from a water-based solution
V. Cloet, J. Feys, R. Hühne, S. Hoste and I. Van Driessche
Page 37

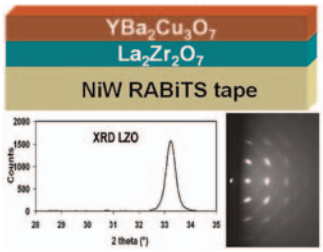

Thin films of La2Zr2O7 (LZO) are produced via a water-based solution, containing metal acetates, acetic acid and triethanolamine. The thin layer is deposited on the textured Ni-5 at%W substrate by dip-coating. The amorphous gel is analysed by HR-TGA/DTA and HR-TEM. The textured layers are analysed by XRD, pole figures, RHEED analysis, AFM and SEM.

Synthesis, structure determination, and infrared spectroscopy of $(NpO_2)_2(SO_4)(H_2O)_4$: Prevalence of cation–cation interactions and cationic nets in neptunyl sulfate compounds
T.Z. Forbes and P.C. Burns
Page 43

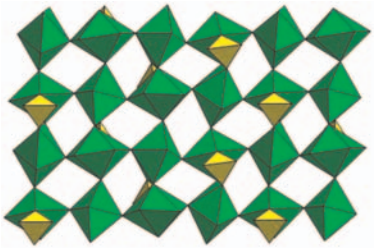

$(NpO_2)_2(SO_4)(H_2O)_4$ was synthesized by hydrothermal methods and its structure determined. A graphical representation of the compound was constructed to facilitate the structural comparison to similar Np^{5+} compounds and the prevalence of the cationic nets in neptunyl sulfate compounds related to the overall stability of the structure is discussed.

Organic–inorganic hybrids constructed by Anderson-type polyoxoanions and copper coordination complexes
Rui-Ge Cao, Shu-Xia Liu, Ying Liu, Qun Tang, Liang Wang, Lin-Hua Xie and Zhong-Min Su
Page 49

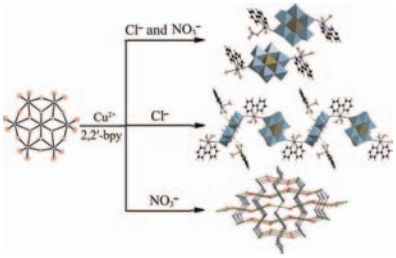

Four organic–inorganic hybrids based on Anderson-type polyoxoanions have been synthesized. Compound **1** displays a discrete structure, **2** shows a chainlike structure, **3** and **4** are isomorphic and exhibit unique 3D open frameworks with lattice waters residing in the channels. The different structures suggest that the overall structures of the compounds are influenced by the nature of the acidic anions.

Transition metal tetramolybdate dihydrates $MMo_4O_{13}\cdot 2H_2O$ (M = Co,Ni) having a novel pillared layer structure
Kazuo Eda, Yu Ohshiro, Noriko Nagai, Noriyuki Sotani and M. Stanley Whittingham
Page 55

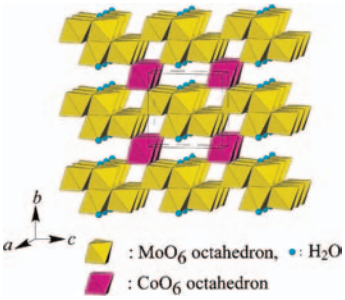

Novel transition metal tetramolybdate dihydrates $MMo_4O_{13}\cdots 2H_2O$ (M = Co,Ni), having an interesting pillared layer structure, were found. The structure was composed of two-dimensional molybdenum-oxide sheets pillared with CoO_6 octahedra. Structural comparison with various tetramolybdates was also made to find a key to structural control.

Mössbauer investigation of ^{57}Fe doped $La_4Ni_3O_{10\pm y}$ phases
M.D. Carvalho, A. Wattiaux, L.P. Ferreira and J.M. Bassat
Page 60

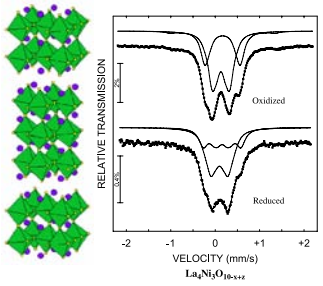

Mössbauer spectra of oxidized and reduced Ruddlesden–Popper compounds $La_4Ni_{2.97}Fe_{0.03}O_{10\pm y}$.

$(NH_4)[V^{III}_{1-x}V^{IV}_xF_{1-x}O_x]$: A new mixed valence vanadium(III,IV) fluoro-arsenate with ferromagnetic interactions and electronic conductivity
Teresa Berrocal, José L. Mesa, José L. Pizarro, Begoña Bazán, Idoia Ruiz de Larramendi, María I. Arriortua and Teófilo Rojo
Page 65

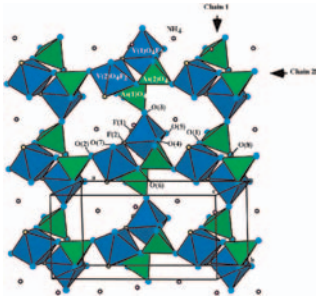

Polyhedral view of the crystal structure of $(NH_4)[V^{III}_{1-x}V^{IV}_x(AsO_4)F_{1-x}O_x]$.

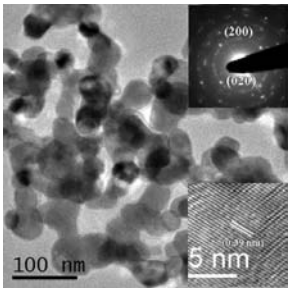

Nanoparticles of ternary metal oxynitrides can be synthesized by means of urea route. Given is the TEM image of the nanoparticles of $CaTaO_2N$ so obtained and the insets show the SAED pattern and HREM image of the nanoparticles.

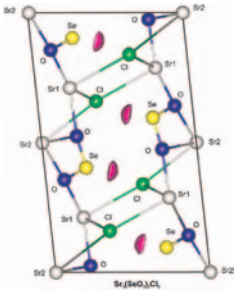

Three new selenite-chlorides $Sr_3(SeO_3)_2Cl_2$ and $Sr_2M(SeO_3)_2Cl_2$ (M = Co,Ni).

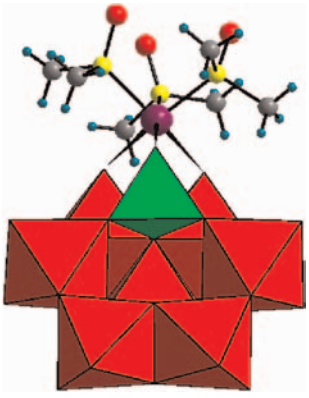

A new tungstoarsenate containing a $Os(dmso)_3$ unit $[HAsW_7O_{28}Os(dmso)_3]^{6-}$ (1) has been synthesized using $[HAsW_9O_{34}]^{8-}$ as polyanion precursor and structurally characterized.

with the Keggin and/or Dawson heteropolymolybdophosphates and PCl_5 in acetonitrile–water solutions via hydrothermal treatment, three new polyoxometalates $X_7[PMo_8O_{30}]$ ($X = Na^+$, 1; K^+, 2; NH_4^+, 3) have been synthesized and characterized. Single crystal X-ray analyses were carried out on $Na_7[PMo_8O_{30}]$ (1) and $(NH_4)_7[PMo_8O_{30}]$ (3). All the three compounds contain the new sandglass-like structure $[PMo_8O_{30}]^{7-}$.

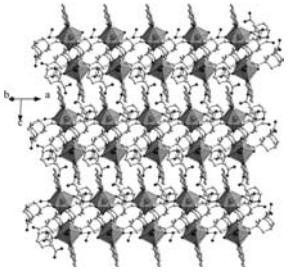

Hydrothermal reactions of 1,10-phenanthroline, 1,3-adamantanedicarboxylic acid and lanthanide choloride yielded a novel supramolecular architectures constructed from polyhedral LnN_2O_6 of distorted bicapped trigonal prism bridged by dicarboxylate.

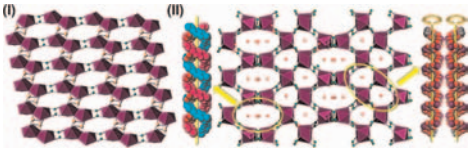

Two new indium(III) compounds have been hydrothermally synthesized and structurally characterized. In **I**, the indium-selenite chains are bridged by oxalate units to form 2D $In_2(SeO_3)_2C_2O_4$ layers. In **II**, the indium atoms are connected through the oxalate units to generate a 3D open framework containing cross-linked 12- and 8-membered ring channels.

Continued

Local structure of Cu in $Cs_8Na_{16}Cu_5Ge_{131}$ type II clathrate
A.N. Mansour, M. Beekman, W. Wong-Ng and G.S. Nolas
Page 107

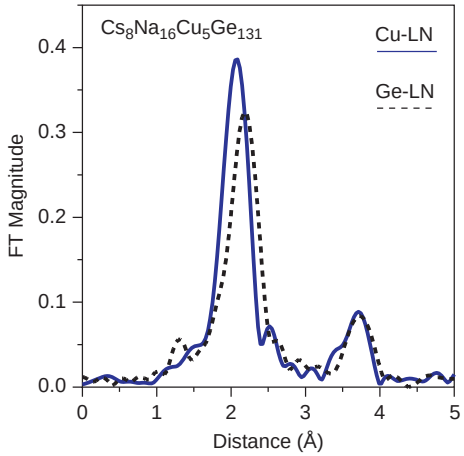

Comparison of Fourier transforms of Cu *K*-edge and Ge *K*-edge EXAFS spectra for $Cs_8Na_{16}Cu_5Ge_{131}$ collected near the temperature of liquid nitrogen (LN). The data clearly show that the Cu–Ge distance is smaller than the Ge–Ge distance, indicating the presence of a local distortion around Cu.

Shape-controlled fabrication of porous ZnO architectures and their photocatalytic properties
Jun Zheng, Zhi-Yuan Jiang, Qin Kuang, Zhao-Xiong Xie, Rong-Bin Huang and Lan-Sun Zheng
Page 115

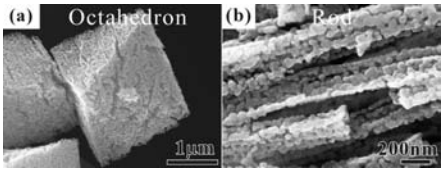

In this paper, we report a simple two-step approach to prepare porous octahedron- and rod-shaped ZnO architectures. The morphology of the porous ZnO nanostructures can be conveniently tailored by controlling the morphologies of the precursor $ZnC_2O_4 \cdot 2H_2O$.

Structure and magnetic properties of rare-earth chromium germanides $RECr_xGe_2$ (RE = Sm, Gd–Er)
Haiying Bie, Andriy V. Tkachuk and Arthur Mar
Page 122

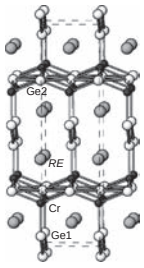

The average structure of $RECr_xGe_2$ corresponds to the $CeNiSi_2$-type, with Cr atoms entering square pyramidal sites. The Cr atoms provide no contribution to the effective magnetic moment in these compounds, which undergo antiferromagnetic ordering below 20 K.

Controlled thermal decomposition of NaSi to derive silicon clathrate compounds
Hiro-omi Horie, Takashi Kikudome, Kyosuke Teramura and Shoji Yamanaka
Page 129

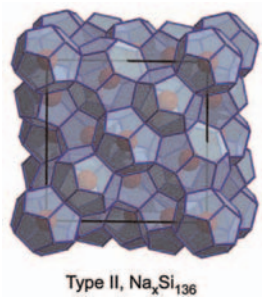

The optimal condition to prepare type II silicon clathrate Na_xSi_{136} with minimal contamination of the type I phase is proposed. The starting NaSi should be thermally decomposed below 440 °C, and the rapid removal of Na vapor evolved is essentially important.

Structural phase transitions in $Zn(CN)_2$ under high pressures
H.K. Poswal, A.K. Tyagi, Andrea Lausi, S.K. Deb and Surinder M. Sharma
Page 136

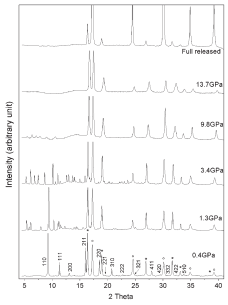

High pressure X-ray diffraction investigations on $Zn(CN)_2$ show three phase transformations i.e., cubic→orthorhombic→cubic-II→amorphous. However, the results strongly depend upon the nature of stress.

Synthesis, structure and physicochemical characterization of a noncentrosymmetric, quaternary thiostannate: $EuCu_2SnS_4$
Jennifer A. Aitken, Jonathan W. Lekse, Jin-Lei Yao and Rosalynn Quinones
Page 141

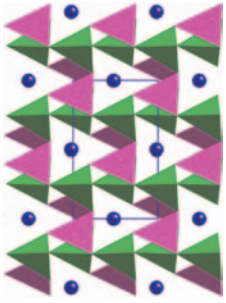

$EuCu_2SnS_4$ crystallizes in the orthorhombic space group *Ama*2 and adopts the $SrCu_2GeSe_4$ structure-type. The structure can be described as a three-dimensional network built from near perfect SnS_4 and distorted CuS_4 tetrahedra together with EuS_8 square antiprisms.

Unusual spin gap transition observed in two new molecular magnets based on $[Ni(mnt)_2]^-$ monoanion (mnt^{2-} = maleonitriledithiolate)

Hong-rong Zuo, Qian Huang, Chun-yan Huang, Dong-hai Huang, Yong Hou, Le-min Yang, Chun-lin Ni and Qing-jin Meng

Page 147

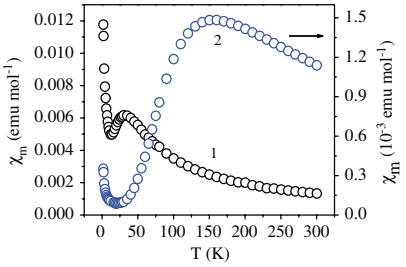

Two new molecular magnets based on $[Ni(mnt)_2]^-$ monoanion form a 1D magnetic chain for **1** and a stepwise stack for **2**, and exhibit unusual spin gap transition.

Crystal and magnetic structures of the brownmillerite compound $Ca_2Fe_{1.039(8)}Mn_{0.962(8)}O_5$

Farshid Ramezanipour, Bradley Cowie, Shahab Derakhshan, John E. Greedan and Lachlan M.D. Cranswick

Page 153

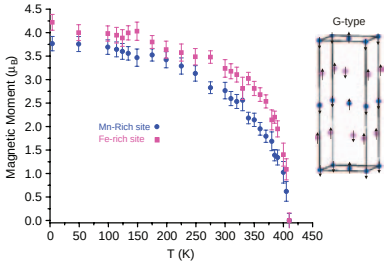

Temperature dependence of the ordered moments at the Mn-rich (octahedral) and Fe-rich (tetrahedral) sites in Ca_2FeMnO_5. The G-type magnetic structure is also shown.

Preparation and spectroscopic characterization of visible light sensitized N doped TiO_2 (rutile)

S. Livraghi, A.M. Czoska, M.C. Paganini and E. Giamello

Page 160

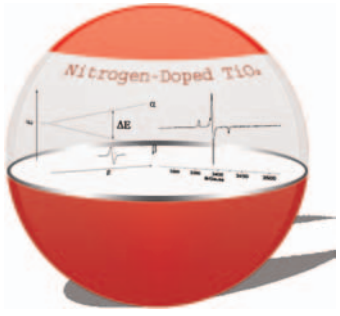

Nitrogen doped TiO_2 represents one of the most promising material for photocatalitic degradation of environmental pollutants with visible light. However, at present, a great deal of activity is devoted to the anatase polymorph while few data about rutile are available. In the present paper we report an experimental characterization of N doped polycrystalline rutile TiO_2 prepared via sol–gel synthesis.

Modulation of the crystallinity of hydrogenated nitrogen-rich graphitic carbon nitrides

Denis Foy, Gérard Demazeau, Pierre Florian, Dominique Massiot, Christine Labrugère and Graziella Goglio

Page 165

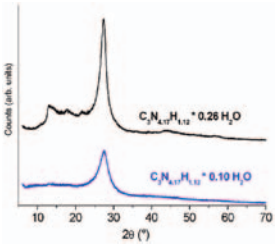

Graphitic hydrogenated nitrogen-rich carbon nitride was synthesized at ambient pressure and mild temperature. The nitrogen overstoichiometry is explained by the presence of triazine voids in the graphene planes. The presence of trapped water molecules into these voids tends to influence the crystallinity and the thermal behavior of the materials.

Characterization and thermal stability of cobalt-modified 1-D nanostructured trititanates

Edisson Morgado Jr., Bojan A. Marinkovic, Paula M. Jardim, Marco A.S. de Abreu and Fernando C. Rizzo

Page 172

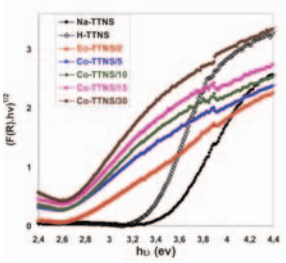

Co^{2+} incorporation in 1D-trititanate crystal nanostructure (Co-TTNS) causes reduction in interlayer distance by comparison with its sodium precursor (Na-TTNS) and leads to enhanced visible light photon absorption efficiency due to a strong band-gap narrowing.

Surfactant-free fabrication of Cu_2O nanosheets from Cu colloids and their tunable optical properties

Yongsong Luo, Youchao Tu, Qinfeng Ren, Xiaojun Dai, Lanlan Xing and Jialin Li

Page 182

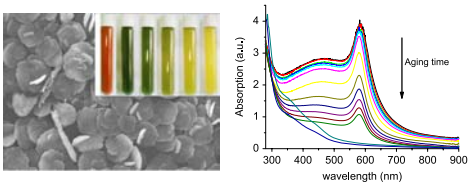

Novel sheetlike Cu_2O 2D nanoarchitectures were successfully synthesized. It was demonstrated that the solvent agent of ethanol played key roles in the formation of the as-synthesized nanosheets.

Continued

Synthesis and structural characterization of $La_xSr_{1-x}MnO_{2.6+\delta}$ ($0.1 < x < 0.4$) compounds displaying compressed octahedral coordination of $Mn^{(4-5x)+}$

Leopoldo Suescun, Bogdan Dabrowski, Steven Remsen and James Mais

Page 187

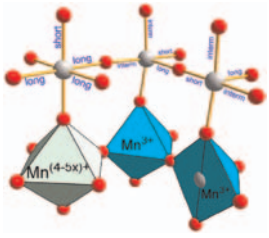

$La_xSr_{1-x}Mn\ O_{2.6}$ compounds ($0.1 \leqslant x \leqslant 0.4$) show a structural phase transition from $Sr_5Mn_5O_{13}$-type oxygen-vacancy-ordering ($x \leqslant 0.3$) to vacancy-disordered $x = 0.4$, showing clear indications of short-range ordering. Compressed MnO_6 octahedra are observed for Mn^{3+}-containing $x = 0.2$ compound that is probably consequence of the presence of elongated MnO_6 octahedra with the long-axis disordered in the x–y plane.

Low-dimensional compounds containing cyano groups. XVII. Crystal structure, spectroscopic, thermal and magnetic properties of $[Cu(bmen)_2][Pt(CN)_4]$ (bmen = *N,N′*-dimethylethylenediamine)

Ivan Potočňák, Martin Vavra, Erik Čižmár, Marcela Kajňaková, Alena Radváková, Dirk Steinborn, Sergei A. Zvyagin, Jochen Wosnitza and Alexander Feher

Page 196

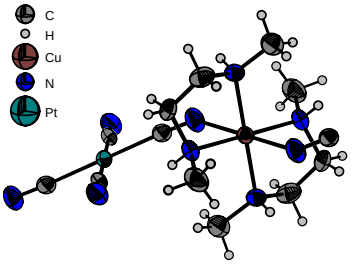

The synthesis, structural analysis, spectroscopic studies, susceptibility and specific-heat measurements of $\{[Cu(bmen)_2][Pt(CN)_4]\}_n$ (*bmen* = *N,N′*-dimethylethylenediamine) are presented. X-ray crystal-structure analysis revealed that the $[Pt(CN)_4]^{2-}$ building blocks are combined with $[Cu(bmen)_2]^{2+}$ units to form a chain-like structure along the *a* axis. The Cu(II) atoms are hexacoordinated by four nitrogen atoms in the equatorial plane belonging to two molecules of bidentate *bmen* ligands with average Cu–N distance of 2.043(18) Å. The axial positions are occupied by two nitrogen atoms from bridging $[Pt(CN)_4]^{2-}$ anions at a longer axial Cu–N distance of 2.490(4) Å. The compound is characterized by the presence of a weak antiferromagnetic exchange coupling $J/k_B = 0.6$ K. Despite the one-dimensional (1D) character of the structure, the analysis of the magnetic properties and specific heat at very low temperatures shows that $[Cu(bmen)_2][Pt(CN)_4]$ behaves as a two-dimensional (2D) square-lattice Heisenberg magnet with weak interlayer coupling.

Rapid Communication

Novel powellite-based red-emitting phosphors: $CaLa_{1-x}NbMoO_8{:}xEu^{3+}$ for white light emitting diodes

Mariyam Thomas, P. Prabhakar Rao, M. Deepa, M.R. Chandran and Peter Koshy

Page 203

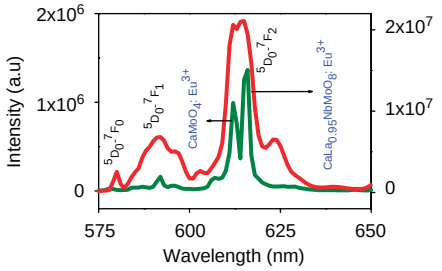

Novel powellite-based red-emitting phosphors: $CaLa_{1-x}NbMoO_8{:}xEu^{3+}$ ($x = 0.01$, 0.03, 0.05, 0.1) have been prepared and characterized for the first time. The photoluminescence investigations indicated that $CaLa_{1-x}NbMoO_8{:}xEu^{3+}$ emits strong red light at 615 nm originating from $^5D_0 \rightarrow {}^7F_2$ (electric dipole transition) under excitation either into the $^5L_0$ state with 394 nm or the $^5D_2$ state with 464 nm. The red emission of $CaLa_{0.95}NbMoO_8{:}0.05Eu^{3+}$ is 10 times stronger than that of $CaMoO_4{:}0.05Eu^{3+}$ under the same excitation wavelength (394 nm).

Author inquiries

For inquiries relating to the submission of articles (including electronic submission where available) please visit this journal's homepage at http://www.elsevier.com/locate/jssc. You can track accepted articles at http://www.elsevier.com/trackarticle and set up e-mail alerts to inform you of when an article's status has changed. Also accessible from here is information on copyright, frequently asked questions and more.
Contact details for questions arising after acceptance of an article, especially those relating to proofs, will be provided by the publisher.

Language services. Authors who require information about language editing and copyediting services pre- and post-submission please visit http://www.elsevier.com/locate/languagepolishing or our customer support site at http://epsupport.elsevier.com. Please note Elsevier neither endorses nor takes responsibility for any products, goods or services offered by outside vendors through our services or in any advertising. For more information please refer to our Terms & Conditions http://www.elsevier.com/termsandconditions

For a full and complete Guide for Authors, please go to: http://www.elsevier.com/locate/jssc

Journal of Solid State Chemistry has no page charges.